density of dislocations within the block. The radial breadth of the spots results from streaking, seen on many photographs (Figs. 4, 5, 7, 9, 11), which has its origin in the stacking faults randomly occurring in the structure during crystal growth (Trigunayat, 1966).

Density of dislocations

If h is the spacing between dislocations in a boundary, the density of dislocations, ϱ, is equal to $1/h$. For small values of θ, $h=b/\theta$. Therefore,

$$\varrho=\theta/b \text{ dislocations cm}^{-1} .$$

The Burgers vector of $a/3\langle 11\bar{2}0\rangle$ dislocations is 4·24 Å and of $a/3\langle 10\bar{1}0\rangle$ dislocations is $4{\cdot}24/\sqrt{3}$ Å in CdI_2 crystals.

Thus the density of dislocations in the boundaries depends directly upon the angle of tilt and hence upon the arc length. It is found to be of the order of 10^5–10^6 dislocations cm^{-1}. The values calculated for a few crystals are listed in Table 1.

The dislocations inside the crystal are considered to be located in the boundaries and inside the blocks, but the number of dislocations inside the block is much less than in the boundaries because the tangential breadth of a spot is generally observed to be much smaller than the arc length.

References

CHADHA, G. K. & TRIGUNAYAT, G. C. (1967). *Acta Cryst.* **22**, 573.

COTTRELL, A. H. (1953). *Dislocations and Plastic Flow in Crystals*. Oxford: Clarendon Press.

FORTY, A. J. (1952). *Phil. Mag.* **43**, 377.

HIRSCH, P. B. (1956). *Progress in Metal Physics*. Vol. 6. London: Pergamon Press.

JAGODZINSKI, H. (1954). *Neues Jahrb. Mineral.* **3**, 49.

SHAW, R., STEADMAN, R. & PUGH, P. D. (1965). *Z. Kristallogr.* **122**, 237.

TRIGUNAYAT, G. C. (1965). *Z. Kristallogr.* **122**, 463.

TRIGUNAYAT, G. C. (1966). *Nature, Lond.* **212**, 808.

TRIGUNAYAT, G. C. & VERMA, A. R. (1962). *Acta Cryst.* **15**, 499.

Acta Cryst. (1969). A**25**, 407

Tilt Boundaries in Single Crystals of Cadmium Iodide. II. Formation of Closed Rings on X-ray Photographs

BY V. K. AGRAWAL AND G. C. TRIGUNAYAT

Department of Physics and Astrophysics, University of Delhi, Delhi-7, India

(*Received* 17 *June* 1968 *and in revised form* 23 *August* 1968)

The X-ray a-axis Laue photographs of single crystals of cadmium iodide grown from solution sometimes show closed rings of various shapes, *viz.* hexagonal, trigonal, *etc.* and of various sizes, corresponding to each X-ray reflexion. They have been satisfactory explained in terms of the formation of more than two tilt boundaries of dislocations during crystal growth. The boundaries result from a vertical alignment of triple nodes of dislocations created by simultaneous slip along close-packed directions. In most cases the slip is confined to the basal planes and occurs at regular intervals.

Introduction

The oscillation and Laue photographs of CdI_2 crystals showing arcing, which consists of an extension of diffraction spots into small arcs, have been discussed in detail in part I (Agrawal & Trigunayat, 1969). This part includes the crystals which show closed rings of various shapes, *viz.* hexagonal, trigonal, *etc.* and of various sizes, on their Laue photographs. Their formation can be adequately explained by postulating the creation of more than two tilt boundaries of dislocations. Similar observations have also been made in single crystals of cadmium bromide grown from solution and will be described later.

Experimental methods

The methods employed for growing the crystals, selecting them, and subjecting them to X-ray examination were the same as described in part I.

Formation of tilt boundaries

Slip along one, or at the most two, close-packed directions at a time was considered in part I. We now consider the possibility of slip simultaneously taking place along the third direction as well. A unit slip on the (0001) basal plane along one of the closest-packed directions, *viz.* $[11\bar{2}0]$, $[\bar{2}110]$, $[1\bar{2}10]$ and their negatives,

gives rise to an edge dislocation, which, as discussed in part I, can be decomposed into two partials as

$$\frac{a}{3}\langle 11\bar{2}0\rangle = \frac{a}{3}\langle 10\bar{1}0\rangle + \frac{a}{3}\langle 01\bar{1}0\rangle .$$

The partials bound a region of stacking fault, the dimensions of which are determined by the condition that the mutual separation of the partials is inversely proportional to the stacking fault energy. The decomposition process amounts to a displacement of an atomic layer, parallel to the (0001) planes, in two stages, first along $\langle 10\bar{1}0\rangle$ and then along $\langle 01\bar{1}0\rangle$. This two-stage displacement, leading to a unit slip, is more probable than a single displacement by one unit along the closest-packed direction because it needs less energy. Indeed, in hexagonal metals it is now well known (Price, 1963) that $a/3\langle 11\bar{2}0\rangle$ dislocations on the {0001} planes are actually made up of two partial dislocations bounding a narrow ribbon of stacking fault. In the hexagonal CdI_2 crystals also we may now regard this as being the actual mode of generation of unit slip.

As a representative case we consider the slip process in the most common CdI_2 polytype, 4*H*. There are two minimal sandwiches in the unit cell, the structure in Zhdanov symbols being described by the layer sequence $(A\gamma B)\,(C\alpha B)$, where A, B, C and α, β, γ, represent the positions of iodine and cadmium ions, respectively. Within a sandwich, *viz.* $(A\gamma B)$ or $(C\alpha B)$, the binding, being ionic in nature, is very strong but the two sandwiches are held together by weak van der Waals forces of attraction. Consequently, as the atomic layers are laid down one after another during crystal growth, slip on an *A* or a *C* layer is far more likely than a slip on a *B* layer. According to the two-stage process of slip discussed above, in completing a unit slip along a closest-packed direction $[11\bar{2}0]$ on an *A* layer, an *A* atom has first to move to an adjacent *C* position and then to the next *A* position (it cannot move to a *B* position as the preceding layer itself happens to be a *B* layer and, according to the rules of close packing of layers, no two neighbouring layers can be identical). It is obvious that there are three such equivalent possibilities, shown by dotted lines in Fig. 1, corresponding to unit slip in three of the six equivalent directions of closest packing, *e.g.* $[11\bar{2}0]$, $[\bar{2}110]$, $[1\bar{2}10]$. Simultaneous slip along these three directions will create three edge dislocations inclined at 120° to each other, forming a triple node on the slip plane, as shown by dotted lines in Fig. 2. Similar slip on a *C* layer but along the other three directions of closest packing, *viz.* $[\bar{1}\bar{1}20]$, $[2\bar{1}\bar{1}0]$, $[\bar{1}2\bar{1}0]$, as shown by solid lines in Fig. 1, will create another triple node of dislocations, rotated through 180° with respect to the first. This is shown by solid lines in Fig. 2. If several triple nodes of one type occur on different basal planes, the strong interaction between dislocations of the same sign will bring them one on top of the other, leading to the formation of a set of three tilt boundaries, inclined at 120° to each other, in planes perpendicular to the slip directions. The boundaries will intersect along a line parallel to the *c* axis and will have essentially the same angle of tilt. The other type of triple nodes will similarly form their own set, giving altogether six boundaries which will divide the crystal into six blocks (Fig. 2). The angle of tilt between two neighbouring blocks will be equal for alternate pairs of neighbouring blocks. These conclusions, although drawn for the particular case of the common type 4*H*, are perfectly general and apply to all polytypes of cadmium iodide, for the basic reason that all CdI_2 polytypes consist of various numbers of identical minimal sandwiches, arranged in various layer sequences, in their unit cells.

Two dislocation-type boundaries can also form. Unit slip on the same basal plane along only two of the three equivalent directions of closest packing will create two intersecting edge dislocations, 120° apart (*cf.* the similar case of twofold slip considered in part I, leading to the formation of composite figures on the X-ray photographs, in which it was tacitly assumed that the two dislocations did not intersect). They will form a quadruple node [Fig. 3(*a*)] which is generally unstable. However, if the scalar product of the Burgers vectors of the two dislocations is negative, the quadruple node can decompose into two triple nodes joined by a third dislocation D_3 [Fig. 3(*b*)]. As shown in Fig. 3, the configuration (*a*) evolves towards (*b*) through the intermediate stage (*c*). This transition results in a release

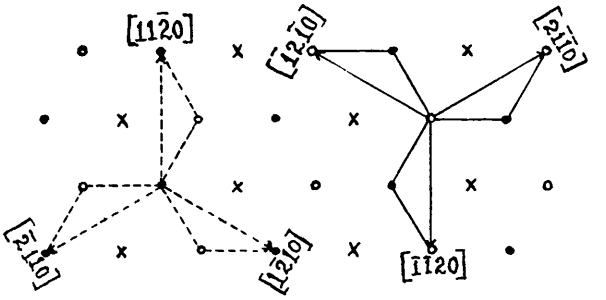

Fig. 1. Slip along close-packed directions. Black circles, cross marks and open circles represent the atoms in *A*, *B* and *C* positions respectively.

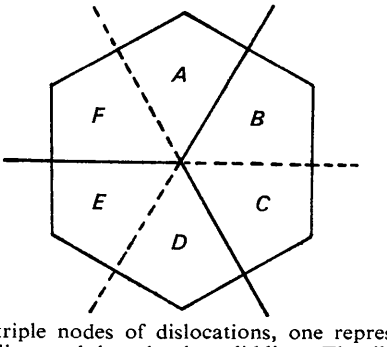

Fig. 2. Two triple nodes of dislocations, one represented by the dotted lines and the other by solid lines. The tilt boundaries along them divide the crystal into six blocks, *A*, *B*, *C*, *D*, *E* and *F*.

of energy for the configuration (Frank, 1955). Once again, a repetition of this process at equal intervals on various basal planes will produce tilt boundaries, having dislocation lines as their axes of tilt, which will divide the crystal into six blocks, A,B,C,D,E,F, as before [Fig. 3(*b*)].

The less favourable slip on a basal plane along the close-packed $\langle 10\bar{1}0\rangle$ directions may also lead to the formation of tilt boundaries. Slip along these directions generates partial dislocations as already discussed in part I. However, the CdI_2 structure will allow slip to occur only along three of these directions, *e.g.* $[10\bar{1}0]$, $[0\bar{1}10]$ and $[\bar{1}100]$, because slip along the other three negative directions brings an A, B, or C layer upon itself, which is prohibited in a close packing of layers. The corresponding partial dislocations, which will now lie along closest-packed directions, will arrange themselves as before to produce three tilt boundaries, making angles of 120° with each other. They will divide the crystal into three blocks, A,B,C (Fig. 4), equally tilted with respect to one another.

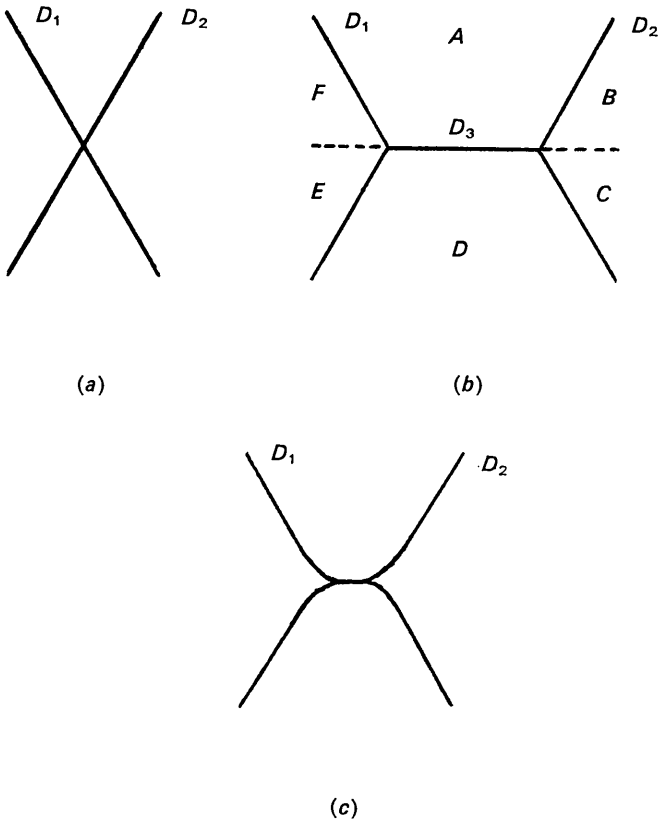

Fig. 3. Intersection of two dislocations D_1 and D_2 (*a*) leading to the formation of two triple nodes (*b*) through the configuration (*c*).

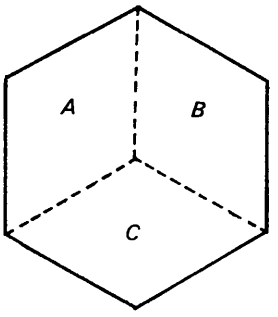

Fig. 4. A triple node of partial dislocations represented by dotted lines. The tilt boundaries along the dislocations divide the crystal into three blocks A, B and C.

Experimental results and discussion

The division of a crystal by tilt boundaries into a number of blocks is confirmed by the formation of closed rings in place of single reflexions on its Laue photograph. According to theory, there should be as many spots at the corners of a ring as there are numbers of blocks. For instance, the division of a crystal into six blocks should give rise to hexagonal rings, each consisting of six spots at the corners. Fig. 5, which is a Laue photograph of crystal No. 1, taken with the *a* axis vertical and the X-ray beam incident in the direction of the *c* axis, provides a good illustration. The intensity-distribution over a ring and its exact shape and size depend on various factors, which will become clear from the following description of some representative cases. The X-ray reflexions on the corresponding *a* axis oscillation photographs are spread into continuous arcs of various descriptions and this effect is also discussed.

(i) Fig. 6, which is a Laue photograph of the lower part of crystal No. 2, shows hexagon-shaped reflexions. It may be usefully compared with Fig. 7, which is a Laue photograph, taken in the same orientation, of a nearly perfect CdI_2 crystal (crystal No. 1 of Part I). Both these photographs were taken with the *a* axis vertical and the angle (referred to as Φ in the following) between the incident X-ray beam and the *c* axis equal to 25°40′, for recording the particularly strong 00.16-reflexion (Fig. 7) isolated from the others. As was discussed in part I, reflexions of high l values are particularly suited for studying the effects of tilt boundary formations. It is seen in Fig. 6 that the hexagonal ring, $A'B'C'D'E'F'$, corresponding to the 00.16 reflexion, has a symmetrical shape, with opposite sides having equal lengths. Its explanation follows from Fig. 3, which depicts the division of a crystal into six blocks, A,B,C,D,E,F, by the formation of two triple nodes joined along the common dislocation line D_3. The exact correspondence between the ring $A'B'C'D'E'F'$ and Fig. 3(*b*) is clear, *e.g.* the blocks A and B give rise to reflexions A' and B' respectively, connected by the strip $A'B'$ between them which originates from the continuous curvature across the intervening boundary of dislocations D_2. Since the boundaries consisting of dislocations D_1 and D_2 have essentially the same angle of tilt and are inclined at 30° to the vertical *a* axis, four sides of the ring, $A'B'$, $C'D'$, $D'E'$, $F'A'$, are of

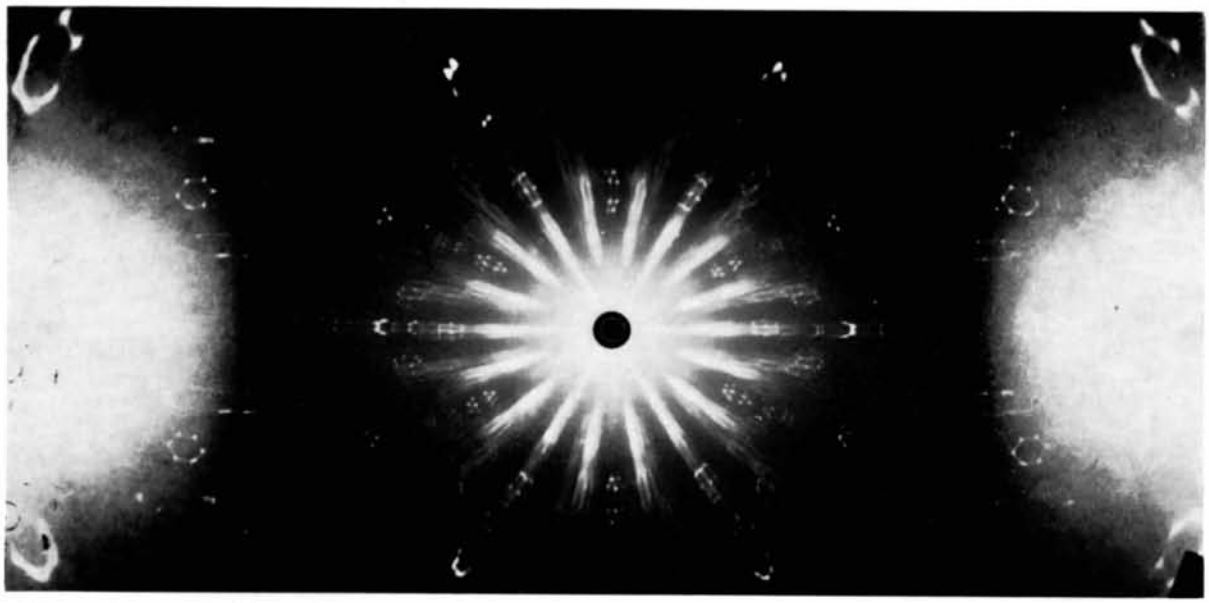

Fig. 5. Laue photograph of crystal No. 1 with the incident X-ray beam in the direction of the c axis ($\Phi=0$). a axis vertical; Cu white radiation; camera radius 3 cm. The crystal is a mixture of polytypes $4H$ and $12R$.

Fig. 6. Laue photograph of lower part of crystal No. 2 with the incident beam inclined to the c axis ($\Phi=25°40'$). Polytype $4H$; other conditions as in Fig. 5.

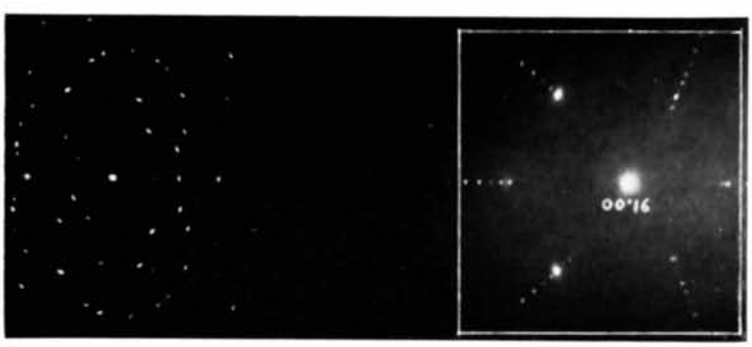

Fig. 7. Laue photograph of crystal No. 1 of Part I. Polytype $4H$; conditions as in Fig. 6. Only the portion within the marked rectangle has been reproduced in Fig. 6 and subsequent corresponding Figures.

[To face p. 409

equal lenths and the angle between any two adjacent sides, $A'B'$ and $B'C'$, $B'C'$ and $C'D'$, $D'E'$ and $E'F'$, $E'F'$ and $F'A'$, is $(90°+\tan^{-1}x/2\sqrt{3})\sim 120°$ [case (ii) of part I]. The other two opposite sides, $B'C'$ and $E'F'$, occurring perpendicular to the central row of reflexions, are also equal, as the same tilt boundary, made up of dislocations D_3, is responsible for their formation. The same boundary gives rise to the long strip joining A' and D'. Upon rotating the crystal through 60° about the c axis, the ring is also rotated through the same angle such that now its other two sides, $A'B'$ and $D'E'$, become perpendicular to the central row (Fig. 8), confirming the angle between any two adjacent sides, to be equal to 120°.

As the c^* directions of the six blocks point in different directions, Bragg's condition, $n\lambda=2d\sin\theta_c$, cannot be simultaneously satisfied for all the blocks, for the characteristic radiation, λ_c. Since the c^* directions of blocks A and D lie in the same vertical plane [case (i) of part I], they will satisfy the Bragg condition for λ_c at the same angle Φ. For this reason, the spots A' and D' of the ring (Fig. 6) are far more intense than the other four spots which arise from weak radiations of other wavelengths and the vertical strip joining the spots A' and D' is also more intense than the strips joining any other two spots. Since the boundaries between the blocks A and F, and blocks E and D are inclined at 30° to the vertical a axis and have the same angle of tilt, θ, the angle Φ is decreased by $\sqrt{3}/2\theta$ [case (ii) of part I] to satisfy the Bragg condition for the blocks E and F, for λ_c. Consequently, it is found that upon decreasing Φ by this magnitude, the spots F' and E' of the ring become stronger than the rest of the spots (Fig. 9). Similarly if the angle Φ is increased by $\sqrt{3}/2\theta$, the spots B' and C', corresponding to blocks B and C, become more intense (photograph not reproduced).

Since the spots on an oscillation photograph arise from characteristic radiation alone, the reflexions from blocks B and F, and blocks C and E, which successively reflect at the same Bragg angle during oscillation, separately overlap, giving rise to only two spots. The blocks A and D give rise to their own separate spots. Thus each reflexion on the oscillation photograph consists of four spots lying along an arc (Fig. 10; *cf.* Fig. 6). Upon rotating the crystal through 60° about the c axis, the angles of tilt of the boundaries inclined at 30° to the a axis, cease to be equal. Consequently, none of the spots overlap during oscillation, so that each reflexion consists of six spots (Fig. 11; *cf.* Fig. 8).

(ii) The Laue photograph of the lower part of crystal No. 3 shows a nearly regular hexagonal ring for the 00.16 reflexion (Fig. 12). The explanation is quite obvious from Fig. 2 which shows the formation of triple nodes of dislocations. If the two types of triple node occur at regular intervals, six boundaries, dividing the crystal into an equal number of blocks, will be formed. Their angles of tilt will be essentially equal. The boundaries perpendicular to the vertical a axis form two sides of the ring of very nearly equal lengths and perpendicular to the central row. The length of either side is nearly equal to $5{\cdot}4\theta$ [case (i) of part I]. The length of any other of the four sides, which arise from the boundaries inclined at 30° to the a axis, is equal to $(\sqrt{3}/2\,.\,2r\theta/\cos\tan^{-1}x/2\sqrt{3})\sim 6\theta$ [cases (ii) and (iv) of part I]. Therefore, all sides of the ring are nearly equal. The angle between any two adjacent sides is almost 120° as in the preceding case. The picture does not change (photograph not reproduced) upon rotating the crystal through 60°, as all the blocks are equally tilted relative to one another. The oscillation photographs (not reproduced) in both orientations showed similar arcs, each consisting of four spots along its length (*cf.* Fig. 10).

In both the crystals (Nos. 2 and 3) it has been observed that if only one block, say A (Fig. 2), is irradiated, only one intense spot is obtained on the Laue photograph (Fig. 13; *cf.* Fig. 12), confirming the division of the crystal into six separate blocks. On account of the divergence of the X-ray beam, the rest of the ring also appears faintly in the photograph.

The upper parts of the two crystals also showed hexagonal rings, similar to those of their lower parts, but the spots on them were elongated towards the centres of the rings, as seen in Fig. 14 which is the Laue photograph of the upper part of crystal No. 3. The elongation follows from a variation in the spacing, h, of dislocation nodes along various parts of the boundaries, resulting in a continuous variation in the θ-value ($\theta=b/h$).

(iii) Hexagonal rings with alternate sides of nearly equal lengths have also been observed. They can arise from a difference in spacings between the two types of triple nodes.

(iv) Fig. 15 is a Laue photograph of the lower part of crystal No. 4 at $\Phi=0$, showing nearly triangular rings. Their formation is quite obvious from Fig. 4, diagrammatically representing the formation of a triple node of partial dislocations. The three sides of a ring are approximately equal [cases (iv) and (v) of part I].

(v) Some Laue photographs show quite irregularly shaped rings. For instance, the Laue photograph of the upper part of crystal No. 5 at $\Phi=0$ (Fig. 16) shows hexagonal rings with unequal sides. The angles between two adjacent sides have arbitrarily different values. To explain these rings, dislocations created by slip along $\langle 10\bar{1}3/n\rangle$ directions on $\{1\bar{1}0n/3\}$ planes, in an nH polytype ($n=2,4,6,\text{---}$), have to be considered. This type of slip will create a dislocation having Burgers vector equal to $\sqrt{c^2/4+a^2/3}\simeq a$. Therefore, from the energy point of view, the creation of such dislocations cannot be neglected. These dislocations may combine with other dislocations, created due to slip along $\langle 10\bar{1}0\rangle$ directions on $\{0001\}$ planes, to form asymmetrical tilt boundaries, having their contact planes inclined to the c axis. They may also interact with other dislocations and create some complicated dislocation network. Neither the angle between the contact plane and the

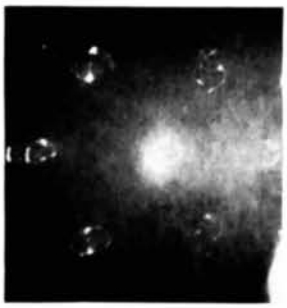

Fig. 8. As Fig. 6 but after rotating crystal through 60° about the *c* axis.

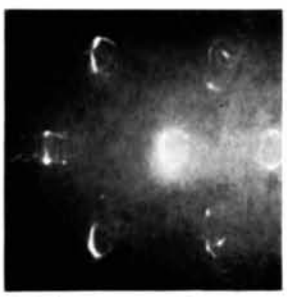

Fig. 9. As Fig. 6 but at $\Phi = (25°40'–1°30')$.

Fig. 10. *a*-axis 15°-oscillation photograph of the lower part of crystal No. 2. Φ varies from 25° to 40°; Cu $K\alpha$ radiation; camera radius 3 cm; polytype 4*H*.

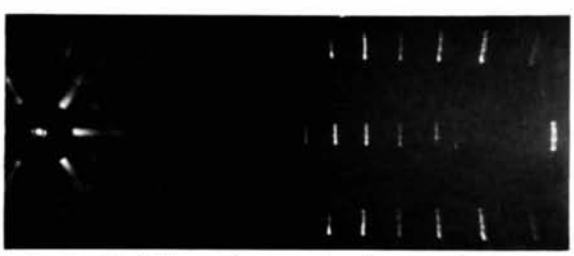

Fig. 11. As Fig. 10 but after rotating the crystal through 60° about the *c* axis.

[*To face p.* 410

Fig. 12. Laue photograph of the lower part of crystal No. 3. Polytype $4H$; conditions as in Fig. 6.

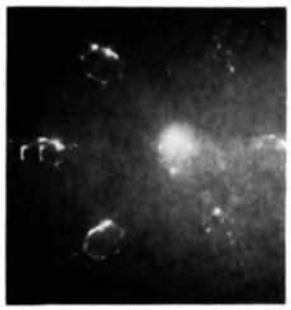

Fig. 13. As Fig. 12 but only block *A* (Fig. 2) is irradiated by the X-ray beam.

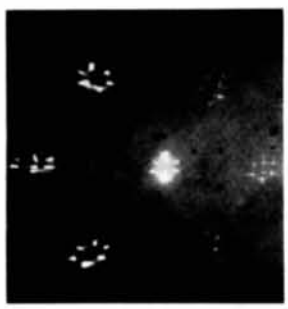

Fig. 14. Laue photograph of the upper part of crystal No. 3. Mixture of polytypes $4H$ and $48R$; conditions as in Fig. 6.

Fig. 15. Laue photograph of the lower part of crystal No. 4. Polytype $4H$; conditions as in Fig. 5.

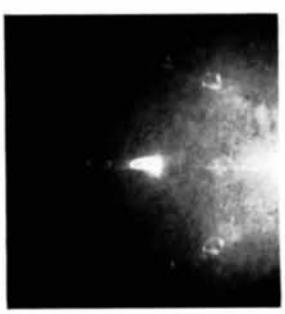

Fig. 16. Laue photograph of the upper part of crystal No. 5. Polytype $4H$; conditions as in Fig. 5.

c axis in the case of asymmetrical tilt boundaries, nor the real nature of interactions between the two types of dislocations is known. Therefore, it is difficult to describe exactly the formation of irregularly shaped rings.

(vi) All the above cases of ring-formations have been discussed for the common CdI_2 polytype 4*H* excepting the upper part of crystal No. 3 which is a mixture of types 4*H* and 48*R*. In addition, rings have also been observed on Laue photographs of other polytypes (photographs not reproduced).

Density of dislocations

The density of dislocations inside the boundaries can be calculated from the X-ray photographs as outlined in part I.

Conclusion

The most significant conclusions emerging from the experimental findings are (*i*) the occurrence of triple nodes of dislocations, created by simultaneous slip along the directions of close packing and (*ii*) the constancy of their spacing in most cases. The latter points to the generation of dislocations at equal intervals during crystal growth. It is noteworthy that the ring-formations have mostly been observed in the lower parts of the crystals, the upper parts usually showing either single spots or only a small amount of arcing. This is to expected because the conditions are favourable for the formation of a large number of dislocations in the initial stages when the saturation is high and the rate of growth is rapid. The phenomenon of ring formation shows that under certain suitable circumstances these dislocations can arrange themselves into highly symmetrical threefold boundaries. Apart from the X-ray methods used by us, electron microscopy can also be profitably employed to reveal the arrangements of dislocations inside the crystals. However, Forty (1960) has observed that CdI_2 crystals decompose under the action of the electron beam.

The authors wish to thank Dr K. D. Chaudhuri for his kind interest and encouragement. One of us (V.K.A.) has received financial support from the Council of Scientific and Industrial Research and the University Grants Commission.

References

AGRAWAL, V. K. & TRIGUNAYAT, G. C. (1969). *Acta Cryst.* A**25**, 401.

FORTY, A. J. (1960). *Phil. Mag.* **5**, 787.

FRANK, F. C. (1955). *Conference on Defects in Crystalline Solids*, p. 159. London: The Physical Society.

PRICE, P. B. (1963). *Electron Microscopy and Strength of Crystals*, p. 41. Ed. G. THOMAS & J. WASHBURN. New York: Interscience.

Acta Cryst. (1969). A**25**, 411

Direct Summation of Madelung Energies

BY J. C. A. BOEYENS AND G. GAFNER

Chemical Physics Group of the National Physical and Chemical Research Laboratories, CSIR, Pretoria, South Africa

(*Received* 12 *August* 1968)

A computerized procedure based on the Evjen method for the direct summation of Madelung energies of centrosymmetric structures is described. The values obtained are strictly according to the definition of the Madelung function and the accuracy depends only on the number of terms taken into consideration. Madelung energies for a variety of structures calculated by this method are compared with values obtained by various other methods.

Introduction

Madelung constants of most simple ionic salts are known accurately, but analyses of the electrostatic interactions in numerous ionic and ion-dipole complexes still have to be made. Methods for the rapid evaluation of the Madelung energies of complicated structures are thus highly desirable and it was surprising to find that almost negligible use has been made of the most obvious methods, *viz.* direct evaluation of lattice sums using computers. Indirect methods which often involve mathematical expressions and correction factors which are much more complicated than the basic equation ($U = -(z\,e)^2\alpha/r$) which defines the Madelung function, are usually employed. The most popular procedure uses the method of Bertaut (1952) with correction factors given by Templeton, 1955 (see also Jones & Templeton, 1956). Evjen (1931) cells are used occasionally together with various devices (Verwey & Heilmann, 1947) to compensate for surface dipoles (de Boer, 1948; Verwey, de Boer & van Santen, 1948). Wood (1959) suggested a method for eliminating